THE ASTROPHYSICAL JOURNAL, 515:465–470, 1999 April 20

TEMPERATURE ANISOTROPIES AND DISTORTIONS INDUCED BY HOT INTRACLUSTER GAS ON THE COSMIC MICROWAVE BACKGROUND

F. ATRIO-BARANDELA
Física Teórica, Universidad de Salamanca, Salamanca 37008, Spain; atrio@astro.usal.es

AND

J. P. MÜCKET
Astrophysikalisches Institut Potsdam, An der Sternwarte 16, D-14482 Potsdam, Germany; jpmuecket@aip.de
Received 1997 December 19; accepted 1998 November 23

ABSTRACT

The power spectrum of temperature anisotropies induced by hot intracluster gas on the cosmic background radiation is calculated. For low multipoles it remains constant, while at multipoles above $l > 2000$ it is exponentially damped. The shape of the radiation power spectrum is almost independent of the average intracluster gas density profile, gas evolution history, or cluster core radii, but the amplitude depends strongly on those parameters. Its exact value depends on the global properties of the cluster population and the evolution of the intracluster gas. The distortion on the cosmic microwave background blackbody spectra varies in a similar manner. The ratio of the temperature anisotropy to the mean Comptonization parameters is shown to be almost independent of the parameters of the cluster model, and at first approximation depends only on the number density of clusters. An independent determination of the contribution of clusters to the distortion of the blackbody spectrum and the temperature fluctuations of the cosmic microwave background would determine the number density of clusters that contribute to the Sunyaev-Zeldovich effect.

Subject headings: cosmic microwave background — cosmology: theory — galaxies: clusters: general

1. INTRODUCTION

The Compton scattering of cosmic microwave background (CMB) photons by the hot gas present in clusters of galaxies was first described by Sunyaev & Zeldovich (1970). The Sunyaev-Zeldovich (SZ) effect has two components: thermal and kinematic. The first is caused by the random thermal motions of the electrons, the distribution of which is assumed to be isotropic (in the cluster reference frame). The kinematic component is an additional effect caused by the peculiar velocity of the cluster with respect to the CMB (see Rephaeli 1995 for a review). At present, several groups are searching for or are setting up telescopes to measure the SZ effect on single clusters (Holzapfel et al. 1997; Jones 1997; Saunders 1997). But apart from the effect of individual clusters, the entire cluster population acts as a screen of scattering sites through which the background photons must pass to reach the observer. The overall effect is both to distort the blackbody spectrum and to induce temperature anisotropies on the CMB. The latter is an important component of the full anisotropy on angular scales of several arcminutes (Cole & Kaiser 1988; Bartlett & Silk 1994; Colafrancesco et al. 1994). The anisotropy depends on the cluster richness, its evolution, and the cosmological model. Therefore, detection of anisotropies and distortions will yield significant insight into the cosmological evolution of clusters.

Analysis of the *COBE*/FIRAS data yielded an upper limit on the degree of Comptonization of the CMB (determined by the parameter $\bar{y}$, to be defined below) of $\bar{y} \leq 1.5 \times 10^{-5}$ at the 95% confidence level (Mather et al. 1994). The PLANCK satellite, scheduled to be launched in the next decade, will not specifically look for distortions. Those will be deduced from the data on temperature anisotropies. At the present stage, several groups are studying methods for subtracting foregrounds (Tegmark & Efstathiou 1996; Hobson et al. 1998) and are performing simulations to predict the sensitivity level at which cosmological parameters can be measured. In this respect, it is necessary to carry out a careful analysis of the power spectrum of the foregrounds, since this will allow us to distinguish at each frequency between the genuine CMB distortions and the contribution of clusters and other foregrounds. As remarked by Tegmark & Efstathiou (1996), this improves the technique of removing foregrounds by comparing data at different frequencies.

In this paper we obtain the radiation power spectrum of CMB temperature anisotropies induced by the entire population of clusters of galaxies, the mean distortion, and the ratio of the temperature anisotropy measured by the Sunyaev-Zeldovich Infrared Experiment (SuZIE) (Church et al. 1997) to the Comptonization parameter. We will show that distortions and temperature anisotropies are related not only for a single cluster but also for the values averaged over all clusters. We extend the work of Bartlett & Silk (1994) and Colafrancesco et al. (1997) by computing the power spectrum and analyzing its dependence with the parameters describing the cluster population and the number density. Contrary to the latter authors, we do not make a detailed analysis of all cosmological models. We restrict our study to the standard cold dark matter (CDM) model.

The outline of the paper is as follows. In § 2, we rederive the power spectrum of the temperature anisotropies due to the contribution of clusters of galaxies. In § 3, we integrate our equations assuming a number density of clusters given by the Press-Schechter formalism. We give the shape of the power spectrum and its dependence on properties of the average SZ cluster population. In § 4, we show that while the amplitude of the radiation power spectrum and the CMB distortion varies strongly with the main cluster

parameters, the ratio of the temperature fluctuation to the mean Comptonization parameter is almost independent of the parameters of the cluster model. In the first approximation, this ratio is determined solely by the number density of clusters. Finally, in § 5 we present our main conclusions.

2. TEMPERATURE ANISOTROPIES INDUCED BY CLUSTERS OF GALAXIES

The passage of CMB photons through a single cluster of galaxies distorts the radiation spectrum by means of inverse Compton scattering. The amplitude of the distortion depends on the frequency. It can be described more appropriately in terms of the change in brightness on the CMB. The temperature difference is given by

$$\frac{\delta T}{T_0} = g(x) y_c \, , \tag{1}$$

where $x = h\nu/k_B T$ is the CMB frequency in dimensionless units and $g(x) = x \coth(x/2) - 4$ gives the frequency dependence of the effect. The cluster Comptonization parameter is defined as

$$y_c = \frac{\sigma_T k_B}{m_e c^2} \int T n \, dl \, , \tag{2}$$

where n and T are the intracluster electron density and temperature, σ_T is the Thomson cross section, k_B is the Boltzmann constant, m_e is the electron mass, and the integral is performed along the line of sight through the cluster.

Clusters are known to be extended X-ray sources with gas-density profiles well fitted by

$$n_e(r) = n_c [1 + (r/r_c)^2]^{-3\beta/2} \, , \tag{3}$$

where n_c is the central electron density and r_c is the core radius of the cluster. The observed values of β, obtained from X-ray surface brightness profiles, range from 0.5 to 0.7 (Jones & Forman 1984; Markevitch et al. 1997). Throughout this paper we will adopt $\beta = 2/3$, since it permits a more simplified treatment.

The distortion induced by the IC gas depends on the temperature profile along the line of sight through the cluster. While most authors assumed the IC gas to be isothermal, in a recent study encompassing 26 nearby *ASCA* clusters, Markevitch et al. (1997) have shown that the gas temperature within clusters decreases slowly with radius. Note that the uncertainty about the *ASCA* point-spread function implies that errors on the density profile of individual clusters are correlated. Therefore, their data can not be used to estimate the average properties of the IC gas. To simplify, we retain the hypothesis of isothermality, since the computation becomes simpler, but our analysis could be easily modified to take into account any dependence of temperature with radius.

If the virial radius of the cluster, r_v, is expressed in terms of the core radius as $r_v = p r_c$, equation (2) can be recast as

$$y_c = y_0 \, \phi(\theta) \, , \tag{4}$$

where $y_0 = (k_B \sigma_T / m_e c^2) r_c \, T n_c$, θ is the angular separation between the line of sight and the center of the cluster, and

$$\phi(\theta) = \frac{2}{\sqrt{1 + (\theta/\theta_c)^2}} \tan^{-1} \sqrt{\frac{p^2 - (\theta/\theta_c)^2}{1 + (\theta/\theta_c)^2}} \, . \tag{5}$$

In this last expression, θ_c is the angle subtended by the core radius of the cluster. Equation (4) gives the effect produced by a single cluster through a particular line of sight. Note that p, given as the ratio between the virial and the core radius, is not a parameter but a function of mass M and redshift z.

2.1. *Mean Comptonization Parameter*

The mean distortion on the CMB induced by all clusters is obtained by adding the effect of one cluster for all possible lines of sight:

$$\bar{y} = \int \frac{dn}{dM} \, dM \, \frac{dV}{dz} \, dz \, \kappa y_0 \, \bar{\phi} \, . \tag{6}$$

In this expression, dn/dM is the cluster number density per unit of mass, and κ gives the probability that a particular line of sight crosses a cluster. This probability is simply $\kappa = (p\theta_c)^2/4$. Finally, $\bar{\phi}$ is the averaged line of sight through a cluster,

$$\bar{\phi} = \frac{\int \phi \theta \, d\theta}{\int \theta \, d\theta} = 4p^{-2}(p - \tan^{-1} p) \, . \tag{7}$$

It is useful to introduce the following notation:

$$\langle \phi \rangle \equiv \frac{1}{2} \int \theta \, d\theta \phi \, . \tag{8}$$

This allows us to write $\kappa \bar{\phi} = \langle \phi \rangle$. Now equation (6) can be rewritten as

$$\bar{y} = \int \frac{dn}{dM} \, dM \, \frac{dV}{dz} \, dz \, y_0 \langle \phi \rangle \, . \tag{9}$$

Note that $\bar{y}$ can now be understood as the average of $y_0 \langle \phi \rangle$ over the entire cluster population. The superposed effect is determined by the cosmological model, cluster abundance, and redshift evolution of the IC medium (Colafrancesco et al. 1997).

2.2. *Radiation Power Spectrum*

The IC gas does not just produce distortions on the CMB spectrum. It also induces temperature anisotropies. The contribution of a single cluster to the temperature anisotropy on a wavenumber $\mathscr{L}$ is

$$\frac{\delta T}{T}(\mathscr{L}) = \frac{1}{2\pi} g(x) y_0 \int d^2\theta \phi(\boldsymbol{\theta}) e^{-i\mathscr{L}\theta} \, . \tag{10}$$

The power spectrum can be obtained by adding in quadrature the contribution of all clusters. Neglecting cluster spatial correlations, we can write (Cole & Kaiser 1988; cf. also Bartlett & Silk 1994)

$$P(l) = \int \frac{dn}{dM} \, dM \, \frac{dV}{dz} \, dz \, [g(x) y_0]^2 \, |\, \tilde{\phi}(l) \,|^2 \, , \tag{11}$$

where $\tilde{\phi}(l)$ is the Fourier transform of the angular profile of the cluster. For scales much larger than the virial radius of a typical cluster, radiation temperature anisotropies originated by the contribution of Poisson distributed clusters lead to $P(l) \simeq$ const.

For scales $l > \theta_c^{-1}$, the behavior of $P(l)$ can be obtained analytically by taking the limit p going to infinity (but keeping $p\theta_c$ finite). In this limit, the radiation power spectrum becomes exponentially damped, that is, it decreases faster than l^4, as predicted by Tegmark & Efstathiou (1996).

In agreement with these authors, we demonstrate numerically that $l^2P(l)$ has a coherence scale, i.e., a maximum, around $l \simeq 1000$–2000. For reference, let us mention that the angular scale $l = 2000$ corresponds to a wavenumber $k \simeq 0.5\,h\,\mathrm{Mpc}^{-1}$, or a scale length of $\lambda \simeq 10\,h^{-1}$ Mpc.

From the power spectrum, we can compute the correlation function of temperature anisotropies. In the flat-sky approximation, it is given by (Atrio-Barandela, Gottlöber, & Mücket 1997)

$$C(\alpha) = \frac{1}{2\pi} \int l\,dl\,W(l)\,P(l)\,J_0(l\alpha)\,, \tag{12}$$

where $W(l)$ represents the window function of the experiment. This expression can be rewritten in a more illuminating form. Replacing the power spectrum (eq. [11]), and after some algebra, for an experiment with infinite resolution and full sky coverage we obtain

$$C(0) = \frac{1}{\pi}\,g(x)^2 \int \frac{dn}{dM}\,dM\,\frac{dV}{dz}\,dz\,y_0^2\langle\phi^2\rangle\,, \tag{13}$$

where ϕ is given by equation (5) and the average is defined in equation (8). This expression states that the correlation function at the origin represents the average of $y_0^2\langle\phi^2\rangle$ over all clusters. For a single cluster, the Compton parameter y_c and temperature anisotropies are related (see eq. [1]). Comparison with equation (9) suggest that a similar relation holds between $[C(0)]^{1/2}$ and $\bar{y}$. In § 4, we show that this is indeed the case. We particularize this relation for the SuZIE experiment (Church et al. 1997), and with the upper limits obtained from their observations we set a constraint on $\bar{y}$ stronger than that derived from *COBE*/FIRAS.

3. CLUSTER MODEL

Numerical estimates of the mean Comptonization parameter, the power spectrum, and the correlation function for a given experiment require that we specify the cluster number density and average properties as a function of mass, redshift evolution of the IC gas, and cosmological model. The number density of clusters per unit of redshift is given by the Press-Schechter formula (Press & Schechter 1974):

$$\frac{dn}{dM} = \sqrt{\frac{2}{\pi}}\,\frac{\rho_b}{M}\,\frac{\delta_v\,b}{\sigma^2}\,\frac{d\sigma}{dM}\exp\left(-\frac{\delta_v^2\,b^2}{2\sigma^2}\right), \tag{14}$$

where ρ_b is the background density at redshift z, M is the virial mass of the cluster, σ is the rms of the linear density fluctuation field at z, smoothed over the region containing M, b is the bias factor, and δ_v is the linear density contrast of a perturbation that virializes at z. The background density and the variance of the density field scale with redshift, $\rho_b \sim (1+z)^3$ and $\sigma \sim (1+z)^{-1}$, while the bias and δ_v are assumed to be constant.

We restrict our analysis to a CDM model with Hubble constant $h = 0.5$ ($H_0 = 100\,h$ km s^{-1}Mpc^{-1}) and normalized to produce a rms matter-density perturbation at an 8 h^{-1} Mpc scale of $\sigma_8 = 0.7$. Only for this particular model and using the largest numerical simulation to date, Tozzi & Governato (1998) checked that for clusters with masses larger than $10^{14}\,M_\odot$, the Press-Schechter formula was in reasonable agreement with the number density of clusters up to redshift $z = 1$ if $\delta_v\,b = 2.1$. A slightly larger value ($\delta_v\,b = 2.6$) was found by Colafrancesco & Vittorio (1994) by fitting the standard CDM model to the observed cluster X-ray luminosity function. The results presented in the next section were obtained assuming the former value at all redshifts.

To compute the temperature anisotropies induced by hot IC gas, we need to translate the properties of a sample of clusters at low redshifts into their equivalents at earlier epochs. In the discussion that follows, the virial mass M will be expressed in units of $10^{15}\,M_\odot$. For the spherical collapse model, the virial radius scales as $r_v = r_{v0}\,M^{1/3}(1+z)^{-1}$, where r_{v0} is the current average virial radius of a $10^{15}\,M_\odot$ cluster. We use the entropy-driven model of cluster evolution developed by Bower (1997) to describe the core-radius evolution as a function of redshift and mass. This model is applicable to an isothermal IC gas distribution. If temperature is proportional to the velocity dispersion of the dark matter, then

$$T = T_g\,M^{2/3}(1+z)\,, \tag{15}$$

where T_g is a normalization constant corresponding to the current temperature of the IC gas of a cluster of $10^{15}\,M_\odot$. In our numerical estimates, we took $T_g = 10^8$ K. The core density evolves as

$$\rho_c \propto T^{3/2}(1+z)^{-3\epsilon/2}\,, \tag{16}$$

where ϵ parameterizes the rate of core-entropy evolution. Therefore, the central electron density scales as $n_c = n_{c0}(T/T_g)^{3/2}(1+z)^{-3\epsilon/2}$. From their study of the luminosity-temperature relation in clusters at high redshift, Mushotzky & Scharf (1997) found $\epsilon = 0 \pm 0.9$.

For a cluster with $\beta = 2/3$, assuming that $r_v \gg r_c$, equation (16) leads to the following expression for the core radius:

$$r_c = r_{c0}\,M^{-1/6}(1+z)^{(-1+3\epsilon)/4}\,, \tag{17}$$

where r_{c0} is the average core radius today for a cluster of $10^{15}\,M_\odot$. From this expression, one obtains $p = p_0\,M^{1/2}(1+z)^{-(3/4)(1+\epsilon)}$. In our numerical estimates, we took $r_{v0} = 1.3\,h^{-1}$ Mpc. The core radius today is given by $r_{c0} = r_{v0}/p_0$. In our analysis we have considered the effect of different core radii, i.e., $p_0 = 7$, 10, and 15, since, according to Makino, Sasaki, & Suto (1998), the core radius of clusters is uncertain and could have been overestimated. Finally, we took the present gas density of a $10^{15}\,M_\odot$ cluster to be $n_{c0} = 2 \times 10^{-3}$ cm^{-3} (Peebles 1993) for a Hubble constant of $h = 0.5$.

We would like to remark that all the relations introduced in this section are to be thought accurate in determining the mean evolution of the cluster population as a whole. They should not be considered applicable to individual clusters.

4. RESULTS AND DISCUSSION

We obtained the power spectrum of temperature anisotropies induced by clusters of galaxies by numerically integrating equation (11). The main limitation of our work is to determine the scale of the less massive objects containing enough hot gas to produce a measurable effect on the CMB. We elaborate on this point further below. Except when otherwise specified, we assumed a lower limit of $M_l = 10^{14}\,M_\odot$, since above that mass scale our cluster model is an adequate description of clusters in the local universe (Mushotzky & Scharf 1997), and the Press-Schechter formula has been found to be accurate (Tozzi & Governato 1998). As an upper limit, we took $M_u = 2 \times 10^{15}\,M_\odot$.

In Figure 1 we plot the mean CMB temperature offset, $T_0[l^2P(l)/2\pi]^{1/2}$. The CMB blackbody temperature, T_0, is expressed in units of μK. We took $g(x) = 1$ in all our plots, so the y-axis should be multiplied by the correct value when comparing with a particular experiment. Note that the mean temperature offset scales as $T_g r_{c0} n_{c0} g(x)$, where the values of all these constants, given in the previous section, correspond to a $10^{15}\ M_\odot$ cluster. In this way, the y-axis in Figure 1 can be easily rescaled to a different set of values. All plots correspond to CDM ($\Omega_B = 0.05$, $H_0 = 50$ km s^{-1} Mpc^{-1}), normalized to $\sigma_8 = 0.7$. In Figure 1*a* we consider the effect of different IC gas evolution histories: $\epsilon = -1$ (*thin solid line*), $\epsilon = 0$ (*thick solid line*), and $\epsilon = 1$ (*dot-dashed line*). In all plots we considered the ratio of virial to core radius to be $p_0 = 10$ at present. In Figure 1*b*, we show the effect of varying the core radius for a fixed virial radius today and no IC gas evolution ($\epsilon = 0$). We considered $p_0 =$ 7, 10, and 15. Note that the amplitude is largest for $\epsilon = -1$ and $p_0 = 7$, since those models lead to larger gas fractions. As expected from our discussion in § 2, all power spectra have a similar bell shape in all cases. The coherence scales are around $l = 1000$–2000. Differences in shape are less important than differences in amplitude. Note also that the dependence is stronger on the core radius than on the IC gas evolution. If our cluster model is correct, by measuring the anisotropy induced by clusters of galaxies, an estimate of the average core radius of the cluster population could be obtained that will only depend marginally on the IC gas evolution.

In Figure 2*a*, we show the power spectrum of temperature anisotropies for different mass cutoffs, $M_l = 10^{13}$, 5×10^{13}, and $10^{14}\ M_\odot$. Note that the amplitude of the power spectrum is remarkably insensitive to the change in the lower limit, the reason being that the integrand of equation (11) is peaked around $2 \times 10^{14}\ M_\odot$ and falls off thereafter, as indicated by Figure 2*b*. In this figure, the left solid line displays $d\bar{y}/dM$, and the dashed and right solid lines show $dP(l)/dM$ for $l = 100$ and $l = 1000$, respectively. As a result, the bulk of the contribution to the radiation power spectrum comes from clusters of mass close to $10^{14}\ M_\odot$. Therefore, even though the entropy-driven model of clusters we used has not been checked for cluster masses below $10^{14}\ M_\odot$, the CMB temperature fluctuations shown in Figure 1 are reasonable accurate. This is not the case for the mean Comptonization parameter $\bar{y}$, which depends strongly on the lower mass cutoff, since the contribution of small-mass clusters dominates the integral, as indicated by Figure 2*b*.

In Figure 3*a*, we plot the mean Comptonization parameter as a function of the IC gas evolution. We varied the lower mass limit of the integral in equation (6). From top to bottom, the thin solid line shows the lower mass limit of $M_l = 10^{13}\ M_\odot$, the dash-dotted line $5 \times 10^{13}\ M_\odot$, and the thick solid line $10^{14}\ M_\odot$, all three with $p_0 = 10$. The upper and lower dashed lines correspond to $p_0 = 7$ and 15, respectively. In the latter two cases, the lower mass limit was $10^{14}\ M_\odot$.

In analogy to the relation given in equation (1), we introduce a new variable η, defined as

$$\eta \equiv \frac{\sqrt{C(0)}}{\bar{y}} . \tag{18}$$

In Figure 3*b*, we plot the behavior of η for the most extreme parameters of the cluster model used. To calculate the correlation function, we used the SuZIE window function. Again, we assumed $g(x) = 1$. Lines correspond to the same models as in Figure 3*a*. The curves corresponding to different lower limits on the mass integral are represented twice. We have plotted η (*lower thin solid and dot dashed lines*) and $\eta(\bar{n}/n_{\rm cl})^{1/2}$ (*upper thin and dashed-dotted lines*). This figure demonstrates that while $C(0)$ and $\bar{y}$ depend strongly on the evolution of the IC gas and the size of the core radius, η varies by less than 20%. The largest dependence of η comes from varying the present number density of clusters. In the

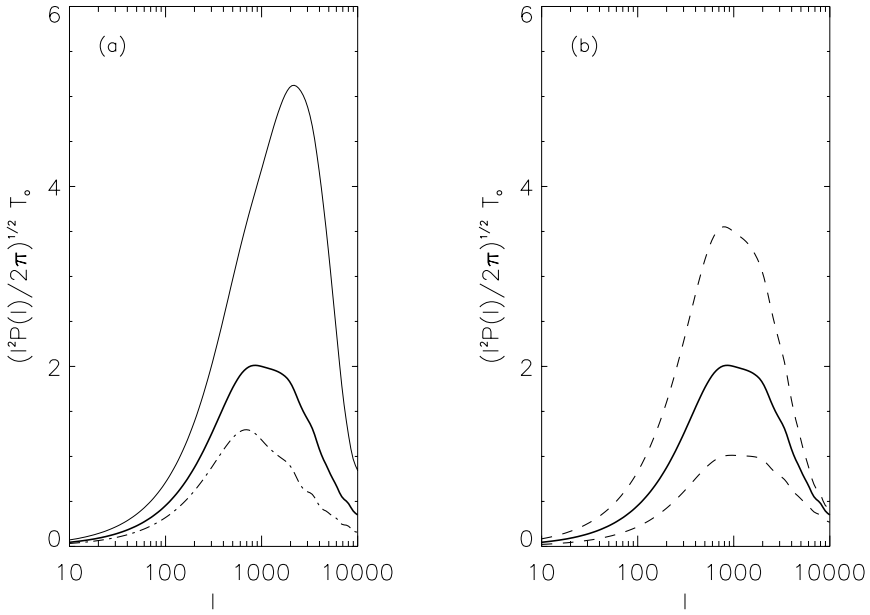

FIG. 1.—Mean CMB temperature offset induced by hot gas in clusters of galaxies, expressed in units of μK. (*a*) Plots corresponding to different gas evolution histories with identical virial-to–core radius ratios today ($p_0 = 10$): *thin solid line*, $\epsilon = -1$; *thick solid line*, $\epsilon = 0$; *dot-dashed line*, $\epsilon = 1$. (*b*) Temperature fluctuations for different ratios of virial-to–core radius today with $\epsilon = 0$: *upper dashed line*, $p_0 = 7$; *thick solid line*, $p_0 = 10$; *lower dashed line*, $p_0 = 15$. Integration of eq. (11) was performed in the mass range $10^{14}\ M_\odot < M < 2 \times 10^{15}\ M_\odot$.

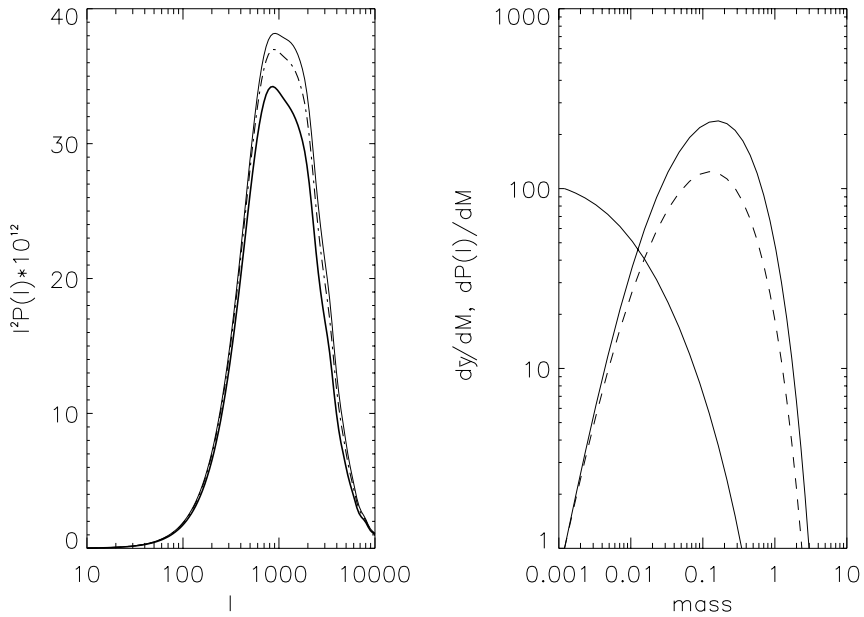

FIG. 2.—*Left*: Power spectrum of CMB temperature anisotropies induced by hot IC gas. The curves differ in their lower limit in the mass integration of eq. (11). *Solid line*, lower limit of $10^{13}\ M_\odot$; *dot-dashed line*, lower limit of $5 \times 10^{13}\ M_\odot$; *thick solid line*, lower limit of $10^{14}\ M_\odot$. The mass upper limit is the same as those of Fig. 1. *Right*: *left solid line*, $d\bar{y}/dM$; *dashed line*, $dP(l)/dM$ for $l = 100$; *right solid line*, $dP(l)/dM$ for $l = 1000$. The scale on the y-axis is arbitrary, and the $d\bar{y}/dM$ curve has been rescaled to fit in the frame.

Press-Schechter theory, decreasing the lower mass limit increases $\bar{n}$, the number density of clusters above a given mass scale. In our case, the lower mass limits $M_l = 10^{13}$, 5×10^{13}, and $10^{14}\ M_\odot$ correspond to 1.5×10^{-3}, 6×10^{-4}, and 2.5×10^{-4} clusters per h^{-3} Mpc^3, respectively. If $C(0)$ and $\bar{y}$ instead of being normalized to σ_8 were normalized to a fixed number of clusters today, the temperature correlation and mean distortion would be rescaled as $C(0)\ n_{\rm cl}/\bar{n}$ and $\bar{y}n_{\rm cl}/\bar{n}$, where $n_{\rm cl}$ is the number density of clusters that produce a measurable effect on the CMB. Then η will scale as $(\bar{n}/n_{\rm cl})^{1/2}$. Going back to Figure 3*b*, the reader can check that this rescaling renders the solid thin and dot-dashed lines in the range of $\eta \simeq 2.0$.

Let us remark that the value of η is different for different experiments. For SuZIE, $\eta \simeq 2.0$, and for an experiment with infinite angular resolution, $\eta \simeq 2.5$ (see eq. [13]). However, a tight relation between distortion and anisotropy exists, independently of the experiment considered.

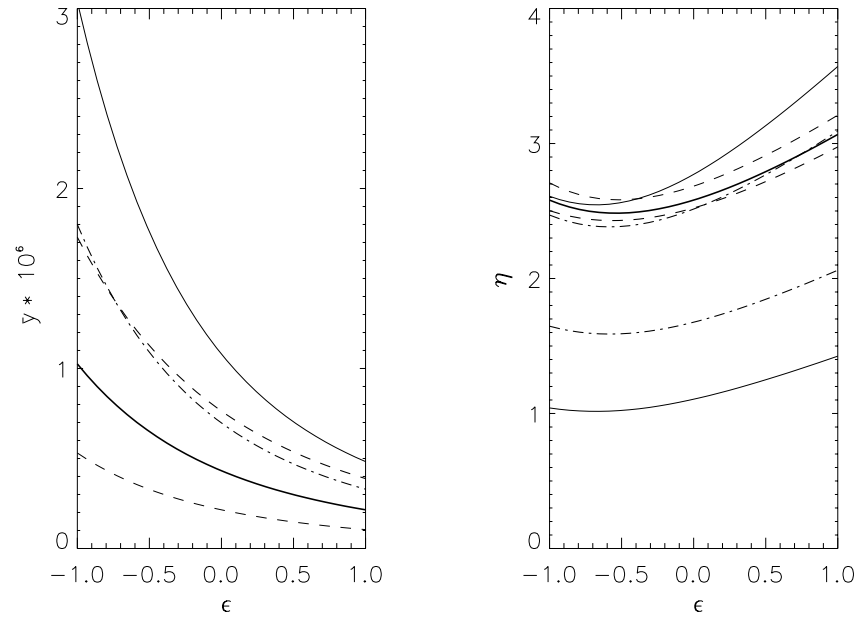

FIG. 3.—*Left*: Mean Comptonization parameter. Thin solid, dot-dashed, and thick solid lines correspond to $p_0 = 10$ and lower limits of mass integration of 10^{13}, 5×10^{13}, and $10^{14}\ M_\odot$, respectively. Upper and lower dashed curves correspond to $p_0 = 7$, 15, and $10^{14}\ M_\odot$ lower limits. *Right*: Ratio of $[C(0)]^{1/2}$ to the mean Comptonization parameter. The two bottom curves correspond to different lower limits on the mass integral (*thin solid line*, $10^{13}\ M_\odot$; *dot-dashed line*, $5 \times 10^{13}\ M_\odot$). In these two cases, the quantity $\eta(\bar{n}/n_{\rm cl})^{1/2}$ was also plotted (*upper thin solid and dot-dashed lines*). We took the number density of SZ clusters to be $n_{\rm cl} = 2.5 \times 10^{-4}\ h^3$ Mpc^{-3}. The upper dashed, thick solid, and lower dashed lines correspond to $p_0 = 15$, 10, and 7, respectively.

This tight relation is a consequence of the insensitivity of the power spectrum to the lower limit of the mass integral.

The upper limits on CMB temperature anisotropies obtained by SuZIE (Church et al. 1997) on angular scales of $l \simeq 2000$ can be used to estimate upper limits on the mean Comptonization parameter that are stronger than those set by *COBE*/FIRAS. Let us assume that temperature anisotropies on scales measured by SuZIE are dominated by clusters, a very conservative assumption for the argument that follows. Using the results summarized in Figure 3*b*, we can impose an upper limit on $\bar{y}$ from the SuZIE upper limit (in absolute value) $[C(0)]^{1/2} \leq 2.1 \times 10^{-5}$ at the 95% confidence level. At 142 GHz (the SuZIE operating frequency), $g(x) \simeq -1$. If we assume that only clusters with masses larger than $10^{14}\ M_{\odot}$ contribute to the CMB distortion, we have $\eta \geq 2.0$. Therefore, $\bar{y} \leq 1.0 \times 10^{-5}$, a constraint stronger than the upper limit obtained by Mather et al. (1994) at the same confidence level. Let us remark that the SuZIE upper limits quoted above were obtained assuming Gaussian statistics, while in our analysis we assumed that clusters were Poisson distributed on the sky. A firm upper bound cannot be obtained without reanalyzing the SuZIE data.

The mean density of clusters can be estimated with independent measurements of distortion and temperature anisotropy. If the contribution of clusters to the temperature fluctuations of the CMB measured by, say, SuZIE, and the blackbody distortion are also determined, comparison with Figure 3*b* would allow a direct estimate of the number density of clusters with IC gas hot enough to produce a significant contribution to the SZ effect. Comparison of the mean number density of SZ clusters with that of X-ray clusters would lead to a better understanding of the IC gas evolution history.

5. CONCLUSIONS

In this paper we have shown that the shape of the power spectrum of temperature anisotropies induced by the hot IC gas is almost independent of model parameters. However, the amplitude does depend on how the mean population of clusters is modeled. As shown by Tegmark (1998), the shape of the power spectrum is important for extracting the foreground contribution on experiments measuring the same region of the sky at different frequencies and angular scales. One could expect the amplitude to be obtained from measurements of temperature anisotropies by experiments such as SuZIE (Holzapfel et al. 1997), Ryle (Saunders 1997), Very Small Array (VSA) (Jones 1997), or the upcomming Microwave Anisotropy Probe (MAP) and PLANCK satellite missions. This will set strong constraints on the average properties of the cluster population.

We showed that a relation between the temperature anisotropy and the mean Comptonization parameter exists on the average, independent of the cluster model and IC gas evolution. The influence of p_0 shown in Figures 1*b* and 3*a* cancels out in the ratio η. In a first approximation, this ratio only varies with the number density of clusters contributing to the SZ effect. This conclusion relies on the assumption that the cluster population as a whole is well described by the scaling relations given in equations (15)–(17). This hypothesis, known as the weak self-similarity principle (Bower 1997), does not imply that these relations should be accurate for single cluster. For example, asphericity is important when computing the effect of a single cluster on the CMB, but it should average out when considering the effect of the whole cluster population. However, if electron clumpiness or temperature gradients are shown to be common in clusters, this would limit the validity of our results. We do not know how to quantify these effects at present, and for this reason we did not include them into our analysis. In addition, let us remark that the influence of different cosmological models through dV/dz has not been addressed in this paper.

To conclude, if our cluster model is applicable to the average cluster population and the number density of SZ clusters is known, then data on temperature anisotropies can be used to determine the distortion of the CMB. On the other hand, two independent measurements of temperature anisotropy and distortion would provide an estimate of the number density of Sunyaev-Zeldovich clusters. Comparison with the number density of X-ray clusters will help us to understand cluster formation and evolution.

We thank the referee for his careful reading of the manuscript that helped to improve the paper substantially. This research was supported by the Spanish German Integrated Actions HA 97/39. F. A. B. would like to acknowledge the support of the Junta de Castilla y León, grant SA40/97.

REFERENCES

Atrio-Barandela, F., Gottlöber, S., & Mücket, J. 1997, ApJ, 482, 1
Bartlett, J. G., & Silk, J. 1994, ApJ, 423, 12
Bower, R. G. 1997, MNRAS, 288, 355
Church, S. E., Ganga, K. M., Ade, P. A. R., Holzapfel, W. L., Mauskopf, P. D., Wilbanks, T. M., & Lange, A. E. 1997, ApJ, 484, 523
Colafrancesco, S., Mazzotta, P., Rephaeli, Y., & Vittorio, N. 1994, ApJ, 433, 454
———. 1997, ApJ, 479, 1
Colafrancesco, S., & Vittorio, N. 1994, ApJ, 422, 443
Cole, S., & Kaiser, N. 1988, MNRAS, 233, 637
Hobson, M. P., Jones A. W., Lasenby, A. N., & Bouchet F. R. 1998, preprint (astro-ph/9806387)
Holzapfel, W. L., et al. 1997, ApJ, 480, 449
Jones, C., & Forman, W. 1984, ApJ, 276, 38
Jones, M. E. 1997, in Proc. XVI Moriond Astrophysics Meeting, Microwave Background Anisotropies, ed. F. R. Bouchet (Gif-sur-Yvette: Editions Frontières), 161
Makino, N., Sasaki, S., & Suto, Y. 1998, ApJ, 497, 555
Markevitch, M., Forman, W. R., Sarazin, C. L., & Vikhlinin, A. 1997, preprint (astro-ph/9711289)
Mather, J. C., et al. 1994, ApJ, 420, 439
Mushotzky, R. F., & Scharf, C. A. 1997, ApJ, 482, L13
Peebles, P. J. E. 1993, Principles of Physical Cosmology (Princeton: Princeton Univ. Press)
Press, W. H., & Schechter, P. 1974, ApJ, 187, 425
Rephaeli, Y. 1995, ARA&A, 33, 541
Saunders, R. 1997, in Proc. XVI Moriond Astrophysics Meeting, Microwave Background Anisotropies, ed. F. R. Bouchet (Gif-sur-Yvette: Editions Frontières), 377
Sunyaev, R., & Zeldovich, Ya. B. 1970, Ap&SS, 7, 3
Tegmark, M. 1998, ApJ, 502, 1
Tegmark, M., & Efstathiou, G. 1996, MNRAS, 281, 1297
Tozzi, P., & Governato, F. 1998, in ASP Conf. Ser. 146, The Young Universe, ed. S. D'Odorico, A. Fontana, & E. Giallongo (San Francisco: ASP), 461